

WAVE-INDUCED ENSTROPY AND DISSIPATION IN A SHEARED TURBULENT CURRENT

Ben R. HODGES⁽¹⁾ and Robert L. STREET⁽²⁾

⁽¹⁾ Centre for Water Research
 University of Western Australia, Nedlands, AUSTRALIA

⁽²⁾ Environmental Fluid Mechanics Laboratory
 Stanford University, California, USA

ABSTRACT

Enstrophy and dissipation produced by turbulent wave-current interactions are analyzed using numerical simulations. Results show vortex stretching beneath the wave trough increases the streamwise enstrophy and the dissipation.

INTRODUCTION

Analysis of interactions between progressive surface waves and a turbulent current requires separating "wave-induced effects" from those due to the current. In laboratory experiments, Cowen (1996) obtained a measure of wave-induced effects by subtracting profiles developed in flows with only a current from profiles developed in wave-current flows. We apply a similar technique to numerical simulations and extend it to develop spatial contours of wave-induced effects. By examining the spatial structure we are able to show that the primary wave-induced effects are due to wave-strains in the streamwise direction which cause stretching of streamwise vortex lines.

NUMERICAL SIMULATIONS

To study the interactions between surface waves and a turbulent current, we use a large-eddy simulation (LES) of the incompressible, unsteady Navier-Stokes equations in three space dimensions with boundary-fitted coordinates. For code details, see Hodges and Street (1997) and Hodges (1997). The code has been validated and shown to be accurate at the scales used here for a number of cases (cf., Zang *et al.*, 1994; Yuan, 1998, Calhoun, 1998; and Hodges, 1997).

In this paper, we present analyses for three wave-current flows and a control case with an open-channel current without a surface wave. Simulations shared the characteristics (non-dimensionalized by friction velocity u_τ and mean water height H) shown in table 1, while those in table 2 were varied. Bulk velocity (U_{bulk}) for the current is defined as:

$$U_{bulk} \equiv \frac{1}{LH} \int_{x=0}^{x=L} \int_{z=0}^{z=\eta} \bar{u} dz dx \quad (1)$$

where L is the domain length, η is the free surface height, and the overbar indicates a spanwise spatial average (used throughout this paper). Bulk and friction velocity Froude numbers and the friction velocity Reynolds number are defined as:

$$Fr_b = \frac{U_{bulk}}{\sqrt{gH}} \quad Fr_\tau = \frac{u_\tau}{\sqrt{gH}} \quad Re_\tau = \frac{u_\tau}{\nu H} \quad (2)$$

The flow boundaries are chosen to match the DNS channel flow of Pan and Banerjee (1995). Their simulations used the same Re_τ as the present work and demonstrated the existence of fully turbulent flow at this Reynolds number.

ak	λ	L	W	Re_τ	U_{bulk}
0.18	2π	2π	π	171	19.2

Table 1: Common characteristics: wave slope (ak), wavelength (λ), domain length (L), domain width (W), Reynolds number (Re_τ), bulk current velocity (U_{bulk})

	Fr_b	Fr_τ	C	T
wave 1	0.64	0.0333	46.5	0.135
wave 2	0.38	0.0192	67.1	0.0937
wave 3	0.21	0.0105	113.	0.0555

Table 2: Varying characteristics: bulk Froude number (Fr_b), friction velocity Froude number (Fr_τ), wave speed (C), wave period (T).

bottom	in/outflow	sides	top
<i>Dirichlet</i>	<i>periodic</i>	<i>periodic</i>	<i>free surface</i>

Table 3: Boundary conditions on simulation domain

Boundary conditions for the simulation domain are shown in table 3. The flow regime is homogeneous in the spanwise direction, allowing instantaneous turbulent statistics to be computed from fluctuations about the instantaneous spanwise mean. Averaging these statistics over the entire simulation provides reasonable estimates of the time-averaged mean statistics for the flow. Because the wave amplitude decays with time, temporal averaging requires detrending techniques (Bendat and Piersol 1986) to remove the effect of the decay.

We limit our analyses to the resolved (*i.e.* grid-scale) enstrophy and dissipation so as to be able to examine individual component effects (which cannot be extracted from the subgrid-scale [SGS] turbulence model). Our estimates suggest that the SGS energy is less than 7% of the total turbulent kinetic energy, which supports our focus on the resolved scales.

WAVE-INDUCED DISSIPATION

The dissipation rate (ϵ) can be written as:

$$\epsilon = \overline{\nu \omega_i \omega_i} + 2\nu \overline{\frac{\partial^2 u_i u_j}{\partial x_i \partial x_j}} \quad (3)$$

Here ω_i and u_i are the fluctuating vorticity and velocity components. The second term on the right of equation (3), the curvature of the Reynolds stress, can generally be neglected (Tennekes and Lumley, 1972). Throughout the flows simulated herein, this term is less than 1% of the local dissipation rate¹. Obtaining a profile of the dissipation in a wave-current flow requires integrating beneath the wave in a suitable stretched coordinate system as described by McDonald (1994) and Cowen (1996). Dissipation profiles for the simulations are shown in figure 1.

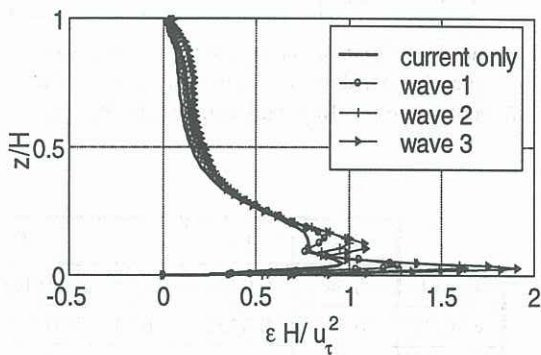


Figure 1: Profiles of dissipation rate.

To examine the effects of wave-current interactions, it is convenient to define a *wave-induced* effect as the difference between a wave-current simulation and a control (current-only) simulation. So, for example, the wave-induced dissipation (ϵ^w) can be defined from the wave-current (ϵ) and current-only (ϵ^c) components:

$$\epsilon^w \equiv \epsilon - \epsilon^c \quad (4)$$

This definition is applied in figure 2 to profile the wave-induced dissipation (normalized by the local dissipation from the current-only simulation).

The flow can be considered to have three distinct regions: (1) the viscous streaming region near the bottom boundary $z/H < 0.25$; (2) the flow core, $0.25 < z/H < 0.9$; and (3) the free surface boundary layer, $z/H > 0.9$. Figure 2 shows that the wave-induced dissipation in the flow core and the free surface boundary layer is significant relative to the local dissipation in the current-only simulation – a result that is not obvious from figure 1.

¹ Not shown due to space limitations.

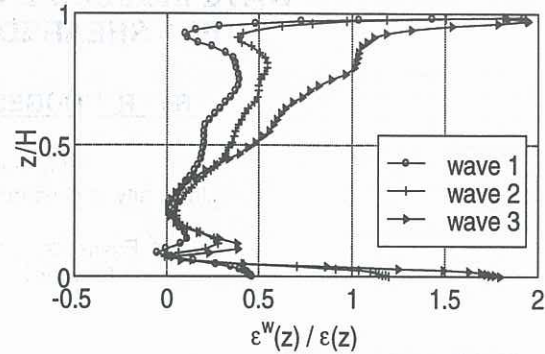


Figure 2: Wave-induced dissipation profiles normalized by local dissipation rate.

Integrating the dissipation data in figure 2 for the three regions (bottom boundary layer, core, free-surface boundary layer), allows us to graph the wave-induced dissipation effect of each term relative the current-only dissipation in the same region. This provides a measure of the local effect of the wave-induced dissipation as shown in figure 3. The dissipation in the free-surface boundary layer is primarily due to the wave rather than wave-current interactions. However, the dissipation in the core region for a wave-only flow² is negligible, so we can infer that the wave-induced dissipation in the core is attributable to the interaction of the wave and the current.

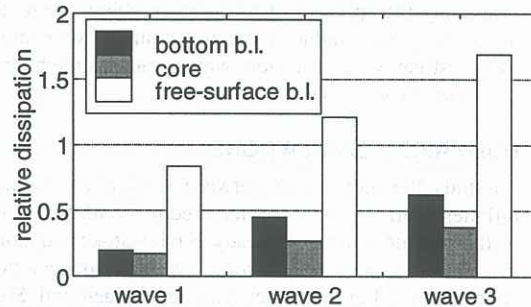


Figure 3: Integrated wave-induced dissipation by region normalized by current-only dissipation by region.

WAVE-INDUCED ENSTROPY

The relationship between enstrophy and dissipation, equation (3), allows us to examine vorticity dynamics that lead to wave-induced dissipation. Profiles of the streamwise and spanwise wave-induced enstrophy components are shown in figures 4 and 5.

The behaviour of the wave-induced streamwise enstrophy is similar for all three waves, showing: (1) generation of streamwise enstrophy within the free surface boundary layer, and (2) a region of enstrophy generation in the upper portion of the flow core ($0.5 < z/H < 0.9$).

For the spanwise enstrophy, figure 5, the spanwise enstrophy generated at the free surface by wave 1 and

² Not shown due to space limitations.

wave 2 remains in the surface boundary layer and is not convected into the flow core. For wave 3 (the fastest wave), the near-surface shear induced by the wave strain is strong enough to convect the spanwise enstrophy from the surface boundary layer into the flow core. The increase in the spanwise enstrophy in the region ($0.4 < z/H < 0.7$) for wave 1 and wave 2 is interesting because it does not appear to be explained either by convection arguments (from boundary layer production) or by the stretching of vortex lines due to wave straining³.

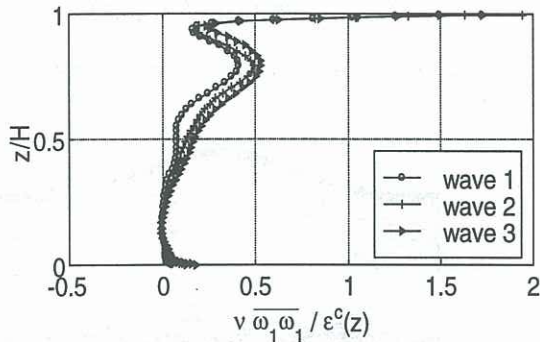


Figure 4: Wave-induced streamwise enstrophy normalized by current-only local dissipation rate

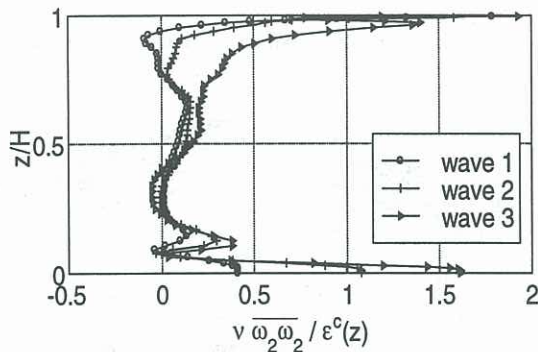


Figure 5: Wave-induced spanwise enstrophy normalized by current-only local dissipation rate

The vertical enstrophy⁴ has only a small effect on the wave-induced dissipation. For the current-only flow the vertical enstrophy and streamwise enstrophy in the region $0.5 < z/H < 0.95$ are of similar magnitudes. From this it might have been reasonable to expect a similarity between the wave-induced vertical and streamwise enstrophies. We observed significant disparities in these terms that can be attributed to different length scales associated with vortex stretching. In the streamwise direction, vortex stretching scales on the wavelength, while for the vertical direction, vortex stretching scales

³A possible explanation is the turning of vortex lines due to horizontal gradients in the "vortex force" produced by cross products of vorticity and velocity. See Tennekes and Lumley, 1972, § 3.3 for a discussion of the vortex force. Vortex turning due to wave-current interactions is being investigated by the present authors.

⁴Not shown due to space limitations.

on the wave height. Thus, streamwise enstrophy is affected to a greater extent than the vertical enstrophy.

WAVE-INDUCED SPATIAL STRUCTURE

The method for computing wave-induced profiles can be extended to computing wave-induced spatial structure. Let x and z be the Cartesian coordinates defining space in the wave-current system, while x^c and z^c are Cartesian coordinates in the current-only system. A set of stretching functions can be defined (McDonald 1994) that maps the coordinates beneath the wave to the coordinates beneath the surface in the current-only flow, such that $x^c = F(x)$ and $z^c = G(z)$. Since our numerical simulation produces discrete data on a unit volume (V) basis, we can write (for example) the wave-induced dissipation⁵ as:

$$\begin{aligned} \epsilon^w(x, z) \equiv & \int_{x-\Delta x}^{x+\Delta x} \int_{z-\Delta z}^{z+\Delta z} \frac{\epsilon(x, z)}{V} dz dx \\ & - \int_{F(x)-\Delta x^c}^{F(x)+\Delta x^c} \int_{G(z)-\Delta z^c}^{G(z)+\Delta z^c} \frac{\epsilon^c(F(x), G(z))}{V} dz dx \end{aligned} \quad (5)$$

This approach accounts for the change in the shape of the domain due to the wave, and is used to develop spatial contour plots of wave-induced enstrophy and dissipation for wave 1 (figures 8 through 11).

Examination of the wave-induced vertical enstrophy, figure 8, shows a balanced effect: vertical stretching of vortex lines beneath the crest increases the enstrophy, while vertical compression beneath the trough decreases the enstrophy⁶. Figure 9 shows that there is strong wave-induced generation of spanwise enstrophy in the boundary layers, and a small reduction just below the free surface boundary layer. The compression and expansion beneath the trough and crest have a small effect in producing/removing spanwise enstrophy. Figure 10 shows the wave-induced streamwise enstrophy. The generation of this term at the free surface is due to the three-dimensional motions of the surface (Hodges and Street, 1997). Within the flow core, vortex stretching beneath the troughs generates streamwise enstrophy, while the crest appears to have little effect.

Comparison of figure 10 with the wave-induced dissipation, figure 11, shows that streamwise vortex stretching is the primary cause of wave-induced dissipation. The small negative region just beneath the crest can be attributed to effects of spanwise enstrophy, while the negative regions in the bottom boundary layer (beneath the troughs) are primarily vertical enstrophy effects, and secondarily spanwise enstrophy effects.

CONCLUSION

This paper demonstrates that dissipation in a turbulent current is increased due to wave-current interactions. Spatial contours of enstrophy components are used to examine the relationships between vortex stretching/compression beneath crests and troughs and

⁵For clarity, Δx and Δz are taken as one-half the grid spacing.

⁶Negative values of wave-induced enstrophy indicate reduction below the enstrophy level in the current-only flow.

increases/decreases in enstrophy components and their contributions to dissipation. The primary effect outside of the boundary layers is a streamwise stretching of vortex lines (which scales on the wavelength) and has a greater effect than the secondary streamwise compression beneath the trough. The vertical stretching/compression of vortex lines (which scales on the wave amplitude) is shown to be balanced beneath the crest and the trough, and thus has little net effect. The contribution of spanwise wave-induced enstrophy is shown to be smaller than the contribution of streamwise enstrophy, but larger than the contribution from vertical enstrophy. At fast wave speeds (relative to the current), convection of spanwise enstrophy from the free surface boundary layer may play an important role.

ACKNOWLEDGMENTS

The simulations in this work were supported by the Fluid Dynamics Program, U.S. Office of Naval Research, Mechanics and Energy Conversion Division, (Program Officer Dr. E.P. Rood, Grant N00014-94-1-0190). The first author would like to thank the Centre for Water Research for its continuing support.

REFERENCES

BENDAT, J.S. and PIERSOL, A.G., *Random Data: Analysis and Measurement Procedures*, Wiley-Interscience, 1986.

CALHOUN, R. *Numerical investigations of turbulent flow over complex terrain*, Ph.D. Dissertation, Dept. of Civil Eng., Stanford Univ., 1998.

COWEN, E.A., *An Experimental Investigation of the Near-Surface Effects of Waves Travelling on a Turbulent Current*, Ph.D. Dissertation, Dept. of Civil Eng., Stanford Univ., 175 pages, 1996.

HODGES, B.R., *Numerical Simulation of Nonlinear Free-Surface Waves on a Turbulent Open-Channel Flow*, Ph.D. Dissertation, Dept. of Civil Eng., Stanford Univ., 235 pages, 1997.

HODGES, B.R., and STREET, R.L., "On simulation of turbulent nonlinear free-surface flows", submitted to *J. Comp. Phys.*, 45 pages, Sept. 1997.

MCDONALD, B.K., *Modeling Laminar Flow Beneath a Prescribed Small-Amplitude Wavy Surface*, Eng. Dissertation, Dept. of Civil Eng., Stanford Univ., 88 pages, 1994.

PAN, Y. and BANERJEE, S., "A numerical study of free-surface turbulence in channel flow." *Phys. Fluids*, 7:1649-1664, 1995.

TENNEKES, H. and LUMLEY, J.L., *A First Course in Turbulence*, The MIT Press, 300 pages, 1972.

YUAN, L.L., and STREET, R.L., "Trajectory and entrainment of a round jet in a crossflow," *Phys. Fluids*, in press, 1998

ZANG, Y., STREET, R.L., and KOSEFF, J.R., "A non-staggered grid, fractional step method for time-dependent incompressible Navier-Stokes equations in curvilinear coordinates," *J. Comp. Phys.*, 114:18-33, 1994.

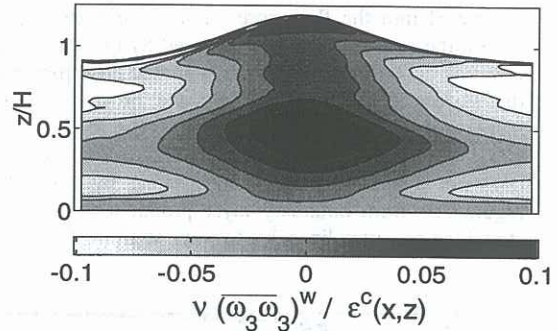


Figure 8: Wave-induced vertical enstrophy

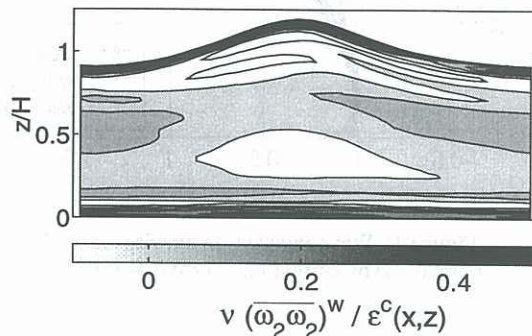


Figure 9: Wave-induced spanwise enstrophy

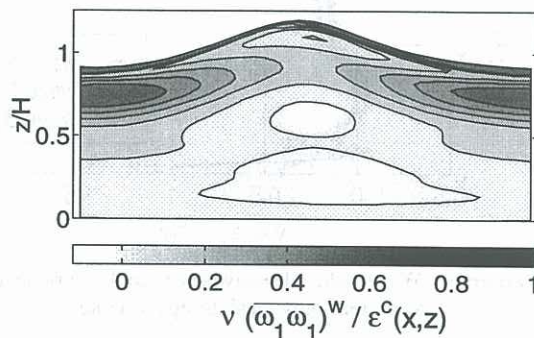


Figure 10: Wave-induced streamwise enstrophy

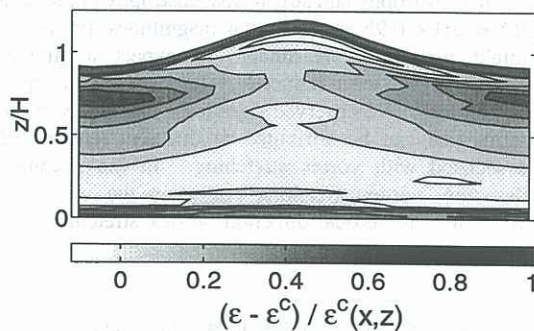


Figure 11: Wave-induced dissipation